ORIGINAL PAPER

physica
status
solidi
www.pss-a.com

Check for
updates

Gettering Mechanism of Copper in n-Type Silicon Wafers

Rie Ozaki,* Kazuhisa Torigoe, Taisuke Mizuno, and Kazuhiro Yamamoto

The dependence of the gettering efficiency for copper impurity in n-type silicon wafers on the concentration of a dopant such as phosphorus, arsenic, or antimony is investigated by chemical analysis of the copper concentration and the observation of copper precipitates. It is found that the gettering efficiency decreases gradually with increasing dopant concentration in the range of 10^{14}–$10^{19}\,\mathrm{cm^{-3}}$ and increases rapidly at concentrations higher than $10^{19}\,\mathrm{cm^{-3}}$. Copper precipitates are observed in the bulk of silicon wafers doped with phosphorus in the concentration range of 10^{14}–$10^{19}\,\mathrm{cm^{-3}}$, suggesting that the relaxation gettering of copper occurs. In contrast, no copper precipitates are observed at concentrations above $10^{19}\,\mathrm{cm^{-3}}$. It is suggested that segregation gettering occurs as a result of the pairing reaction between copper and heavily doped phosphorus. It is concluded that the gettering mechanism of copper in n-type silicon wafers changes from relaxation gettering to segregation gettering with increasing dopant concentration.

1. Introduction

Metal impurities such as copper, iron, and nickel in silicon wafers have a detrimental impact on the performance and yield of semiconductor devices. Therefore, various studies have been conducted on gettering techniques to remove metal impurities from the active region of devices, and gettering techniques using oxide precipitates,[1–9] polysilicon back seal (PBS),[5,10,11] ion implantation,[12–14] and shallow dopants in silicon[15–20] have been developed over the past few decades. In general, gettering mechanisms are divided into two types, relaxation gettering[2,21] and segregation gettering.[22,23] Relaxation gettering involves the formation of metal precipitates. For example, oxide precipitates can act as the preferred nucleation sites for supersaturated metal impurities such as copper, iron, and nickel in silicon during the cooling process after heat treatment.[2,5,21,24,25] In contrast, segregation gettering depends on the difference in solid solubility between two regions with and without gettering sites. Boron, which is used for the p-type shallow doping of silicon, is an effective gettering site via the formation of pairs of boron with metal impurities.[15–19] For example, copper and iron are strongly gettered in heavily boron-doped wafers.[15,18,19] However, studies on

the gettering effect of n-type doping are fewer than those on the effect of boron doping. In general, n-type silicon wafers doped with phosphorus, arsenic, or antimony are used for power devices such as insulated gate bipolar transistors (IGBTs) and metal oxide semiconductor field-effect transistors (MOSFETs), which have recently made rapid progress in terms of capacity enlargement and the reduction of transmission loss.[26] To improve the gettering techniques for these devices, it is critical to understand the effect of doping on the gettering mechanism in n-type silicon wafers.

Although several studies on the relationship between n-type dopants and copper contamination have been carried out,[15,19,20,27] the gettering mechanism in n-type silicon remains unclarified. For example, Istratov et al. proposed that relaxation gettering occurs by copper precipitation in n-type silicon.[27,28] Hoelzl et al. reported that copper gettering occurred at n-type dopant concentrations above $3 \times 10^{19}\,\mathrm{cm^{-3}}$,[19] and Shabani et al. indicated that copper was gettered at phosphorus concentrations above $1 \times 10^{19}\,\mathrm{cm^{-3}}$[20] in the case of copper contamination levels of 1×10^{12} and $1.7 \times 10^{13}\,\mathrm{cm^{-2}}$, respectively. Although they suggested that segregation gettering occurs due to the binding of copper and n-type dopants,[19,20] the effect of relaxation gettering due to copper precipitates or oxide precipitates in such heavily doped silicon has not been clarified.

In this study, to reveal the gettering mechanism of copper, the gettering competition between the wafer surface and the bulk of n-type silicon was investigated using silicon wafers doped with phosphorus, arsenic, or antimony at concentrations ranging from 10^{14} to $10^{20}\,\mathrm{cm^{-3}}$. The wafers were pretreated by rapid thermal annealing (RTA) to remove oxide precipitate nuclei. The dependence of the gettering efficiency for copper contamination of $1 \times 10^{13}\,\mathrm{cm^{-2}}$ on the dopant concentration was determined from depth profiles of the copper concentration obtained by chemical analysis after the drive-in annealing of copper. In addition, it was found by the observation of copper precipitates that the gettering mechanism changes with the dopant concentration.

2. Experimental Section

2.1. Sample Preparation

n-Type silicon wafers (200 mm) were prepared from Czochralski silicon crystals doped with phosphorus, arsenic, or antimony at concentrations ranging from 10^{14} to $10^{20}\,\mathrm{cm^{-3}}$. The specifications of the silicon wafers investigated are summarized in **Table 1**. All wafers were pretreated by RTA in argon ambient

R. Ozaki, Dr. K. Torigoe, T. Mizuno, K. Yamamoto
Technology Division
Advanced Evaluation and Technology Development Department
SUMCO Corporation
1-52 Kubara, Yamashiro-cho, Imari, Saga 849-4256, Japan
E-mail: rozaki@sumcosi.com

The ORCID identification number(s) for the author(s) of this article can be found under https://doi.org/10.1002/pssa.201900220.

Table 1. Specifications of silicon wafers used in this work. The oxygen concentration was estimated using the old ASTM (1976) conversion factor of 4.815×10^{17} cm^{-2}.

Dopant	Dopant concentration [cm^{-3}]	Resistivity [Ω cm]	Oxygen concentration [$\times 10^{17}$ cm^{-3}]
P	3.2×10^{14}	10.4	12.6
P	1.5×10^{15}	3.1	13.6
P	6.0×10^{15}	0.8	13.1
P	4.5×10^{18}	0.01	10.9
P	6.0×10^{19}	0.001	9.8
As	2.3×10^{19}	0.003	10.9
As	3.3×10^{19}	0.002	9.5
As	5.2×10^{19}	0.001	8.2
Sb	2.4×10^{18}	0.02	12.0

at 1150 °C for 1 min to exclude the gettering effect of oxide precipitates formed during the crystal growth of silicon. The front surfaces of the wafers were uniformly contaminated with copper by spin coating[29] at 1×10^{13} cm^{-2}. After spin coating, copper on the surface was introduced into the bulk of the wafers by drive-in annealing in nitrogen ambient in a horizontal furnace at 900 °C for 30 min. After the drive-in annealing, the wafers were pulled from the furnace at a rate of 100 mm min^{-1}. The average cooling rate was estimated at 50 K min^{-1}.

2.2. Evaluation of Density of Oxide Precipitates

After RTA, the wafers were cleaved. To estimate the gettering effect of oxide precipitates in the n-type silicon wafers used in this work, etch pits were observed under an optical microscope at cleaved surfaces that were etched to a depth of about 2 μm in Wright etchant[30] after further annealing at 1000 °C for 16 h.

2.3. Chemical Analysis of Depth Profiles of Copper Concentration

Copper concentrations of the wafers after the drive-in annealing were analyzed by inductively coupled plasma mass spectrometry (ICP-MS) and atomic absorption spectrometry (AAS). A mixture of 2% hydrofluoric acid (HF) and 2% hydrogen peroxide (H$_2$O$_2$) was used to recover the copper from the front and back surfaces for copper concentration determination by ICP-MS.[31] Depth profiles of the copper concentration in the bulk region near the front and back surfaces (0–5 μm in depth) were obtained by AAS analysis in combination with the layer etching method of sample preparation, in which a mixture of 38% HF and 68% nitric acid (HNO$_3$) solutions was used.[31] The concentration of copper remaining in the bulk after the layer etching was measured by ICP-MS in combination with the bulk decomposition method.[31]

2.4. Observation of Copper Precipitates

The dependence of copper precipitation on the dopant concentration was investigated using phosphorus-doped silicon wafers

(phosphorus concentrations: 3.2×10^{14} to 6.0×10^{19} cm^{-3}). After the drive-in annealing, the density of copper precipitates in the bulk of the wafers was measured by IR light scattering tomography (LST).[32] The scattering intensity, which is proportional to the volume of copper precipitates, was also obtained.[33] As IR scattering from precipitates hardly occurs in heavily doped wafers due to IR absorption in the bulk, the etch pits considered to be related to copper precipitates were also observed under an optical microscope at cleaved surfaces that were etched to a depth of about 2 μm with Wright etchant.[30] In addition, to detect small copper precipitates that cannot be detected as etch pits, a transmission electron microscopy (TEM) sample of the wafer doped with phosphorus at a concentration of 6.0×10^{19} cm^{-3} was prepared using a focused ion beam. TEM observation was carried out along the [001] direction at an acceleration voltage of 200 kV. The detection limit (DL) for precipitate density estimated from an observation area is 1×10^{10} cm^{-3}.

3. Results

3.1. Evaluation of Density of Oxide Precipitates

The density of oxide precipitates in all wafers after RTA was lower than the DL of 5.0×10^{7} cm^{-3}.

3.2. Copper Gettering Efficiency

Figure 1 shows the copper concentrations on the front and back surfaces of all wafers after the drive-in annealing at 900 °C for 30 min. The copper concentration on the back surface after the drive-in annealing is almost equal to that on the front surface, indicating that all the copper contaminating the front surface diffused into the bulk of the wafer during the drive-in annealing and out-diffused to both wafer surfaces during the cooling process. Hall and Racette reported that solid solubility of copper in n-type silicon depends on dopant concentrations.[15] The reported values of solid solubility are above 10^{15} cm^{-3} at even 700 °C. Therefore, copper contaminated on the wafer surface can uniformly dissolve into the bulk with the concentration of 1×10^{14} cm^{-3} during the drive-in annealing at 900 °C as mentioned earlier. The copper concentrations on the front and back surfaces of silicon wafers heavily doped with phosphorus at a concentration of 6.0×10^{19} cm^{-3} and arsenic at a concentration of 5.2×10^{19} cm^{-3} were found to be lower than those at other doping levels. **Figure 2** shows the depth profiles of copper concentration in the wafers doped with phosphorus at concentrations of 4.5×10^{18} cm^{-3} (Figure 2a) and 6.0×10^{19} cm^{-3} (Figure 2b) after the drive-in annealing. Figure 2a,b shows that the copper concentration in the bulk including the near surface region of 0–5.0 μm depth doped with phosphorus at a concentration of 6.0×10^{19} cm^{-3} (Figure 2b) is higher than that doped at 4.5×10^{18} cm^{-3} (Figure 2a), resulting in the lower concentration of copper at the wafer surfaces, as shown in Figure 1. The copper detected in the bulk heavily doped with phosphorus is considered to be gettered in the bulk as a result of gettering competition between the wafer surfaces and the bulk during the drive-in annealing. It is noted in Figure 2 that in the heavily doped wafer (phosphorus concentration: 6.0×10^{19} cm^{-3}) the near surface

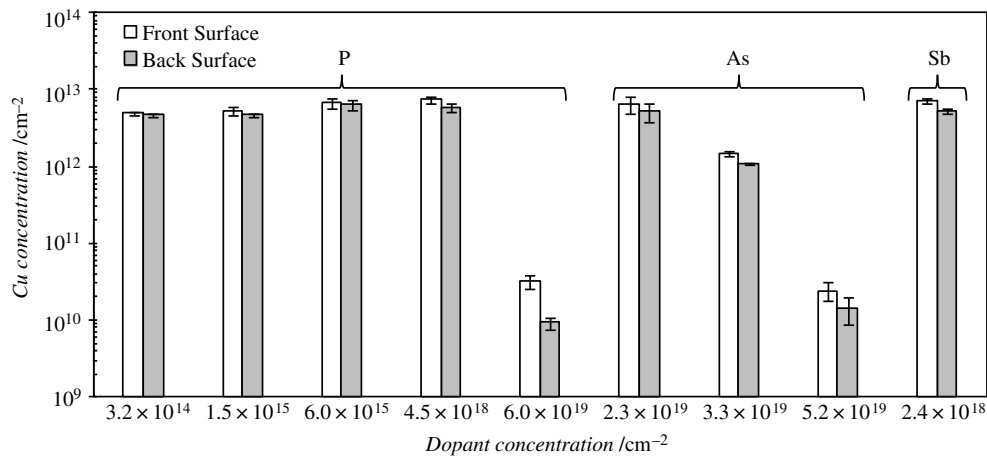**Figure 1.** Concentrations of copper on the front and back surfaces after drive-in annealing at 900 °C for 30 min.
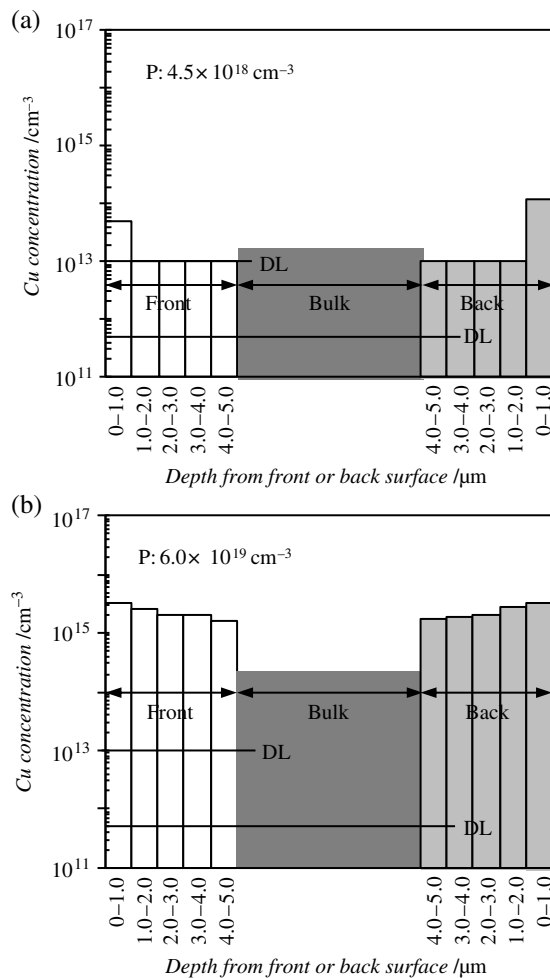

Figure 2. Depth profiles of copper concentration after drive-in annealing at 900 °C for 30 min. The phosphorus concentrations in silicon wafer are a) 4.5×10^{18} cm^{-3} and b) 6.0×10^{19} cm^{-3}. The DLs of the layer etching and bulk decomposition methods are 1.0×10^{13} and 5.0×10^{11} cm^{-3}, respectively.

region of 0–1.0 μm depth shows really high copper concentration above 1×10^{15} cm^{-3} compared with the lightly doped wafer (phosphorus concentration: 4.5×10^{18} cm^{-3}). Such a high copper concentration in the near surface region used for a critical device area has a detrimental impact on the performance and yield of semiconductor devices; therefore, an epitaxial wafer in which copper can be gettered from a lightly doped epitaxial layer into a heavily doped silicon substrate as reported by Hoelzl et al.[19] should be used for the fabrication of semiconductor devices. In this analysis, the gettering efficiency η is defined as the fraction of the copper concentration detected in the bulk (C_{bulk})

$$\eta\,(\%) = \frac{C_{\mathrm{bulk}}}{C_{\mathrm{all}}} \times 100 \qquad (1)$$

where C_{all} is the total concentration of copper in each sample measured by chemical analysis. Here, C_{bulk} is defined as the sum of the copper concentration of the near surface region in 0–5.0 μm depth and the bulk region. The higher gettering efficiency η means that the value of C_{bulk} is higher than the copper concentration in the wafer surface as a result of gettering competition between the wafer surface and the bulk including the near surface region. The contamination level of other metal impurities such as iron, nickel, and aluminum measured by the chemical analysis is lower than that of copper by two orders of magnitude, indicating that the contamination of other metal impurities can be neglected in this work.

Figure 3 shows the dependence of the gettering efficiency for copper on the dopant concentration. The gettering efficiency is about 9% in an antimony-doped silicon wafer (dopant concentration: 2.4×10^{18} cm^{-3}). In phosphorus-doped silicon wafers, the gettering efficiency decreases gradually with increasing dopant concentration in the range from 10^{14} to 10^{19} cm^{-3}. However, the gettering efficiency increases sharply at phosphorus and arsenic concentrations of 6.0×10^{19} and 3.3×10^{19} cm^{-3}, respectively. As shown in Figure 3, there is no significant difference in gettering efficiency among the three dopants.
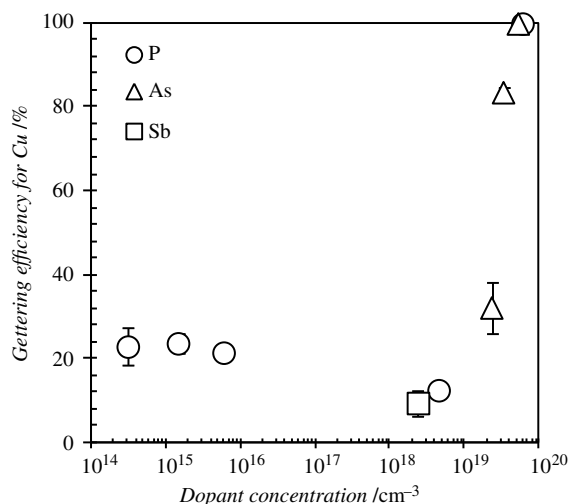
Figure 3. Dependence of the gettering efficiency for copper on the dopant concentration in phosphorus-doped silicon wafers (circles), arsenic-doped silicon wafers (triangles), and an antimony-doped silicon wafer (square).

3.3. Dependence of Copper Precipitation on Dopant Concentration

Figure 4 shows the density and scattering intensity of defects measured by LST and the densities obtained by the observation of etch pits after preferential etching. They are attributed to copper precipitates because neither defects nor etch pits are observed in wafers, which are not contaminated with copper. The results obtained by LST indicate that the density of copper precipitates increased and the size of the copper precipitates decreased with increasing dopant concentration in the range of 3.2×10^{14} to $6.0 \times 10^{15} \, \mathrm{cm}^{-3}$. No copper precipitates were observed because of IR absorption at phosphorus concentrations
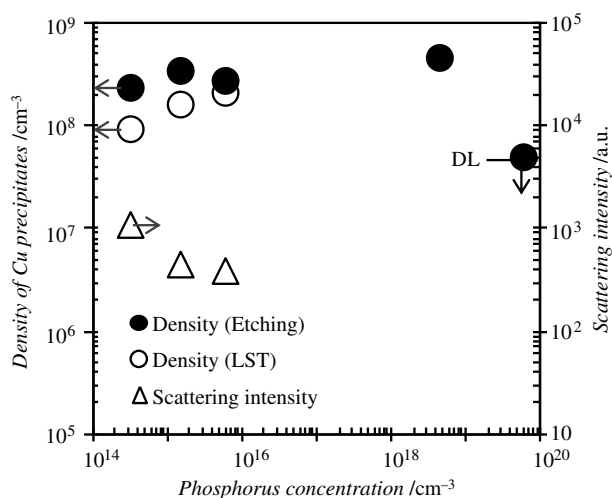

Figure 4. Density (circles) and scattering intensity (triangles) of copper precipitates in the bulk of phosphorus-doped silicon wafers after drive-in annealing at 900 °C for 30 min. The filled and open circles show the measurement results obtained by preferential etching and LST, respectively. The DL of preferential etching is $5.0 \times 10^7 \, \mathrm{cm}^{-3}$.

of 4.5×10^{18} and $6.0 \times 10^{19} \, \mathrm{cm}^{-3}$. The observation of etch pits showed that the density of copper precipitates increases with increasing phosphorus concentration from 3.2×10^{14} to $4.5 \times 10^{18} \, \mathrm{cm}^{-3}$. However, no copper precipitates were observed in the wafer with a phosphorus concentration of $6.0 \times 10^{19} \, \mathrm{cm}^{-3}$. TEM observation also did not reveal any precipitates in the wafer with a phosphorus concentration of $6.0 \times 10^{19} \, \mathrm{cm}^{-3}$.

4. Discussion

4.1. Gettering Effect of Oxide Precipitates

Relaxation gettering efficiency of oxide precipitates depends on the density and size of oxide precipitates.[24,25] Hoelzl et al. reported the relationship between the gettering efficiency for copper and the normalized inner surface of oxide precipitates ($4\pi NR^2d$,[24] where N and R are the density and radius of oxide precipitates, respectively, and d is the wafer thickness.) The gettering efficiencies of oxide precipitates in all the wafers used in this study were estimated from the experimental results of the density after further annealing at 1000 °C for 16 h and the calculated platelet diagonal length after the drive-in annealing. The growth rate of platelet precipitates was calculated assuming that the growth reaction is limited by oxygen diffusion in silicon with an aspect ratio of 0.01.[34] **Table 2** shows the radius and the normalized inner surface of oxide precipitates. Note that R is defined as the radius of a spherical precipitate with the same volume as a platelet precipitate. To estimate the normalized inner surface of oxide precipitates ($4\pi NR^2d$), we assumed that the density of oxide precipitates (N) is $5.0 \times 10^7 \, \mathrm{cm}^{-3}$ at the DL. The values of $4\pi NR^2d$ calculated using the wafer thickness $d = 725 \, \mu\mathrm{m}$ are summarized in Table 2. The gettering efficiencies for copper of oxide precipitates were less than 5% in all wafers, which were determined by considering the dependence of the gettering efficiency on $4\pi NR^2d$ reported by Hoelzl et al.,[24] indicating that the gettering effect of oxide precipitates can be neglected in this work.

4.2. Gettering Mechanism of Copper in n-Type Silicon Wafers

When metal impurities such as copper, iron, and nickel contaminate the surfaces of silicon wafers, they diffuse into the bulk of

Table 2. Radius and normalized inner surface ($4\pi NR^2d$) of oxide precipitate after RTA.

Dopant	Dopant concentration [cm^{-3}]	Radius of oxide precipitate (R) [nm]	$4\pi NR^2d$
P	3.2×10^{14}	6.3	1.8×10^{-5}
P	1.5×10^{15}	6.8	2.1×10^{-5}
P	6.0×10^{15}	6.6	2.0×10^{-5}
P	4.5×10^{18}	5.3	1.3×10^{-5}
P	6.0×10^{19}	4.5	9.2×10^{-6}
As	2.3×10^{19}	5.3	1.3×10^{-5}
As	3.3×10^{19}	4.1	7.7×10^{-6}
As	5.2×10^{19}	2.9	3.8×10^{-6}
Sb	2.4×10^{18}	5.9	1.6×10^{-5}

the wafers during heat treatment due to their high solubility and diffusivity in silicon. During the cooling process after heat treatment, supersaturated metal impurities out-diffuse to wafer surfaces. If gettering sites exist in the bulk of the wafers, metal impurities are gettered in the bulk. In general, the gettering mechanisms are divided into two types, relaxation gettering[2,21] and segregation gettering.[22,23] Relaxation gettering occurs due to the formation of metal precipitates when the concentration of metal impurities in silicon is supersaturated, resulting in a decrease in the metal concentration to a level corresponding to the solid solubility of the metal. In contrast, segregation gettering depends on the difference in solid solubility between two regions with and without gettering sites. In segregation gettering, the concentration of a metal in the region without gettering sites could decrease below a level corresponding to the solid solubility of the metal. It is necessary to take into account the solid solubility, diffusion, and precipitation of metal impurities to understand the gettering mechanism.

Copper dissolves in silicon in a positively charged state in the form of an interstitial configuration (Cu_i^+). The donor level of copper is considered to lie very close to or above the conduction band edge of silicon.[35] Since the Fermi level approaches the conduction band with increasing dopant concentration in n-type silicon wafers, Hall and Racette suggested that the solid solubility of copper decreases gradually up to a dopant concentration of 10^{19} cm^{-3} due to the decreasing ionization rate of Cu_i^+.[15] In contrast, the solid solubility increases rapidly because of the ionization of substitutional copper (Cu_s^{3-}) when the phosphorus concentration is above 10^{19} cm^{-3}.[15] This trend of the solid solubility of copper agrees with the dependence of the gettering efficiency for copper on the phosphorus concentration, as shown in Figure 3, indicating that the gettering mechanism of copper is determined by the dependence of the charge state of copper on the Fermi level position.

At phosphorus concentrations from 3.2×10^{14} to 4.5×10^{18} cm^{-3}, more small high-density copper precipitates were detected with increasing dopant concentration, as shown in Figure 4. Istratov et al. reported that the density of copper precipitates in n-type silicon strongly depends on a cooling rate after heat treatment.[36] After the rapid cooling of 2000 K s^{-1}, the density of copper precipitates is estimated to be 10^{12} cm^{-3}, and the slow cooling rate of 200 K s^{-1} results in the low precipitate density of 10^9 cm^{-3}.[36] The slower cooling rate of 0.8 K s^{-1} in this study leads to the lower precipitate density of 10^8 cm^{-3} as shown in Figure 4. In general, the formation of precipitates is divided into two stages, nucleation and growth. First, precipitate nuclei are generated. After that, precipitates grow because diffusing species aggregate to the precipitate nuclei.[34] It is considered that the increase in the density of copper precipitates at phosphorus concentrations from 3.2×10^{14} to 4.5×10^{18} cm^{-3} is caused by the increase in their nuclei due to the high supersaturation of copper because the solid solubility of copper decreases with increasing dopant concentration, as shown by the experimental results reported by Hall and Racette.[15] Istratov and Weber suggested that copper nuclei are negatively charged in n-type silicon and that Cu_i^+ aggregates at the nuclei by the Coulomb force; as a result, the size of copper precipitates increases.[27] Therefore, the growth of copper precipitates is suppressed due to the

decrease in the concentration of Cu_i^+, which depends on the shift of the Fermi level position as mentioned earlier.

Hoelzl et al. calculated the solid solubility of copper in phosphorus-doped wafers as a function of the doping level at different temperatures on the basis of the following reactions[19]: the distribution of interstitial or substitutional copper

$$Cu_i^0 + V \leftrightarrow Cu_s^0 \tag{2}$$

the distribution of copper in differently charged states

$$Cu_i^0 \leftrightarrow Cu_i^+ + e^- \tag{3}$$

$$Cu_s^0 + 3e^- \leftrightarrow Cu_s^{3-} \tag{4}$$

and pairing reaction

$$Cu_s^{3-} + P_s^+ \leftrightarrow (CuP)_s^{2-} \tag{5}$$

As shown in Equation (2), copper in the electrically neutral charge state in silicon is divided into one of the two types, interstitial copper (Cu_i^0) or substitutional copper (Cu_s^0). Some of the Cu_i^0 atoms change to Cu_s^0 atoms through their interactions with vacancies (V). Equation (3) and (4) show that copper in n-type silicon exists as Cu_i^+ and Cu_s^{3-}. Hoelzl et al. reported that the gettering efficiency for copper increases in heavily phosphorus-doped silicon because the solid solubility of copper increases due to the reaction between copper and the dopant.[19] That is, segregation gettering occurs by the pairing reaction of Cu_s^{3-} with positively charged substitutional phosphorus (P_s^+), as shown in Equation (5).[19] According to first principles calculation, such pairing reaction is stable because the binding energy between substitutional copper and substitutional phosphorus is 3.41 eV.[37] The change in solid solubility calculated by Hoelzl et al., considering the pairing reaction of Cu_s^{3-} and P_s^+ agrees with the dependence of the solid solubility on the dopant concentration experimentally determined by Hall et al.[15,19]

No copper precipitates are observed at a phosphorus concentration of 6.0×10^{19} cm^{-3}, indicating that copper in silicon is unsaturated. According to the solid solubility of copper calculated by Hoelzl et al.,[19] it is found that the copper contamination level of 1×10^{14} cm^{-3} in this work is unsaturated at temperatures above about 100 °C. In contrast, relaxation gettering occurs due to copper precipitates in the phosphorus concentration range from 3.2×10^{14} to 4.5×10^{18} cm^{-3} as shown in Figure 4. The solid solubility of copper calculated by Hoelzl et al.[19] shows that the contaminated copper in this study is supersaturated at temperatures below 400 °C. These results suggest that the precipitation temperatures of copper in phosphorus-doped silicon range from 100 to 400 °C. Ramappa and Henley reported that copper in p-type silicon precipitates below 150 °C.[38] In contrast, copper in n-type silicon is expected to precipitate at higher temperatures than 150 °C because copper precipitates readily occur in n-type silicon by the Coulomb force between negatively charged copper precipitates and Cu_i^+ as mentioned earlier.[27] The precipitation temperatures of copper should also depend on copper concentration, a cooling rate, and vacancy concentration after RTA. Seibt and Graff reported that the size and morphology of copper precipitates depend on copper concentration,[39] and Istratov et al. indicated that the density of copper precipitates in n-type silicon
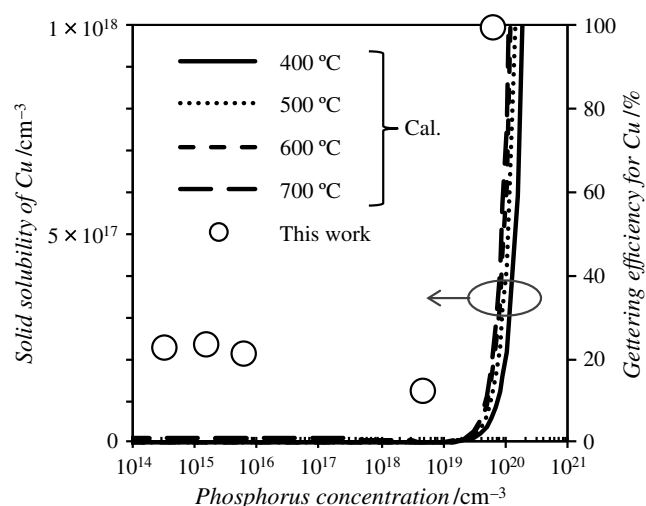
Figure 5. Dependences of the solid solubility and gettering efficiency of copper on phosphorus concentration. The circles show the gettering efficiency experimentally obtained in this work. The solid, dotted, short-dashed, and long-dashed lines are the solid solubilities at 400, 500, 600, and 700 °C, respectively, which are calculated on the basis of the chemical reactions in Equation (2)–(5).

changes by a cooling rate after heat treatment,[36] suggesting that their precipitation temperatures depend on copper concentration and a cooling rate. The composition of copper precipitates in silicon is considered to be metal-rich Cu_3Si.[40] Because of their volume expansion in the silicon matrix, emission of silicon self-interstitials or absorption of vacancies plays an important role for copper precipitation.[39] Therefore, their precipitation temperatures should also depend on vacancy concentration remaining after RTA at 1150 °C for 1 min performed in this study.

Figure 5 shows the phosphorus concentration dependences of the solid solubility of copper calculated on the basis of the chemical reactions in Equation (2)–(5) proposed by Hoelzl et al.[19] and the gettering efficiency experimentally obtained in this work. As shown in Figure 5, the solid solubility increases rapidly at phosphorus concentrations above 10^{19} cm^{-3} similar to the gettering efficiency, indicating that segregation gettering occurs due to the binding of Cu_s^{3-} and P_s^+. In conclusion, the gettering mechanism of copper in n-type silicon wafers changes from relaxation gettering to segregation gettering with increasing dopant concentrations. The relaxation gettering efficiency due to copper precipitates (12.4–23.6%) is very low compared with the segregation gettering efficiency (99.7%), as shown in Figure 3.

5. Conclusion

The dependence of the gettering efficiency for copper on the concentrations of different dopants was investigated using n-type silicon wafers pretreated by RTA to exclude the gettering effect of oxide precipitates formed during the crystal growth of silicon. The results showed that the gettering efficiency decreased gradually with increasing dopant concentration in the range from 10^{14} to 10^{19} cm^{-3}, and increased sharply at dopant

concentrations above 10^{19} cm^{-3}. This trend reflects the dependence of the solid solubility of copper in n-type silicon wafers on the dopant concentration, as experimentally determined by Hall et al., and there was no significant difference in the gettering efficiency among phosphorus, arsenic, and antimony. Copper precipitates were observed in the bulk of wafers doped with phosphorus in the concentration range of 10^{14}–10^{19} cm^{-3}, indicating that relaxation gettering occurred due to the copper precipitates formed during the cooling process after heat treatment. However, the gettering efficiency due to copper precipitates was not very high (12.4–23.6%). In contrast, our results suggest that segregation gettering occurred due to the pairing reaction between Cu_s^{3-} and P_s^+ in heavily phosphorus-doped wafers, in which no copper precipitates were observed (phosphorus concentration: 6.0×10^{19} cm^{-3}). This study revealed that the gettering mechanism of copper in n-type silicon wafers changes from relaxation gettering to segregation gettering with increasing dopant concentration.

Conflict of Interest

The authors declare no conflict of interest.

Keywords

[1] H. Tsuya, K. Tanno, F. Shimura, *Appl. Phys. Lett.* **1980**, *36*, 658.
[2] D. Gilles, E. R. Weber, S. K. Hahn, *Phys. Rev. Lett.* **1990**, *64*, 196.
[3] R. Falster, W. Bergholz, *J. Electrochem. Soc.* **1990**, *137*, 1548.
[4] R. J. Falster, G. R. Fisher, G. Ferrero, *Appl. Phys. Lett.* **1991**, *59*, 809.
[5] S. Ogushi, S. Sadamitsu, K. Marsden, Y. Koike, M. Sano, *Jpn. J. Appl. Phys.* **1997**, *36*, 6601.
[6] G. Kissinger, D. Kot, M. Klingsporn, M. A. Schubert, A. Sattler, T. Müller, *ECS J. Solid State Sci. Technol.* **2015**, *4*, N124.
[7] G. Kissinger, D. Kot, M. A. Schubert, A. Sattler, T. Müller, *Solid State Phenom.* **2016**, *242*, 236.
[8] Y. Zeng, X. Ma, J. Chen, W. Song, W. Wang, L. Gong, D. Tian, D. Yang, *J. Appl. Phys.* **2012**, *111*, 033520.
[9] M. Porrini, V. V. Voronkov, A. Giannattasio, *ECS Trans.* **2018**, *86*, 73.
[10] M. B. Shabani, T. Yoshimi, S. Okuuchi, T. Shingyoji, in *Crystalline Defect and Contamination, PV 97–22* (Eds: B. O. Kolbesen, P. Stallhofer, C. Claeys, F. Tardiff), The Electrochemical Society Proceedings Series, Pennington, NJ, USA **1997**, p. 318.
[11] M. B. Shabani, K. Hirano, Y. Shiina, T. Kihara, T. Shingyoji, *Solid State Phenom.* **2005**, *108–109*, 385.
[12] O. Kononchuk, R. A. Brown, Z. Radzimski, G. A. Rozgonyi, F. Gonzalez, *Appl. Phys. Lett.* **1996**, *69*, 4203.
[13] R. A. Brown, O. Kononchuk, G. A. Rozgonyi, S. Koveshinikov, A. P. Knights, P. J. Shimpson, F. González, *J. Appl. Phys.* **1998**, *84*, 2459.
[14] K. Kurita, T. Kadono, R. Okuyama, S. Shigematsu, R. Hirose, A. Onaka-Masada, Y. Koga, H. Okuda, *Phys. Status Solidi A* **2017**, *214*, 1700216.
[15] R. N. Hall, J. H. Racette, *J. Appl. Phys.* **1964**, *35*, 379.
[16] W. Wijaranakula, *J. Electrochem. Soc.* **1993**, *140*, 275.

[17] P. A. Stolk, J. L. Benton, D. J. Eaglesham, D. C. Jacobson, J. Y. Cheng, J. M. Poate, S. M. Myers, T. E. Haynes, *Appl. Phys. Lett.* **1996**, *68*, 51.

[18] S. A. Mchugo, R. J. McDonald, A. R. Smith, D. L. Hurley, E. R. Weber, *Appl. Phys. Lett.* **1998**, *73*, 1424.

[19] R. Hoelzl, K.-J. Range, L. Fabry, *Appl. Phys. A* **2002**, *75*, 525.

[20] M. B. Shabani, T. Yamashita, E. Morita, *Solid State Phenom.* **2008**, *131–133*, 399.

[21] M. Aoki, A. Hara, A. Ohsawa, *J. Appl. Phys.* **1992**, *72*, 895.

[22] L. Baldi, G. F. Cerofolini, G. Ferla, G. Frigerio, *Phys. Status Solidi* **1978**, *48*,523.

[23] J. S. Kang, D. K. Schroder, *J. Appl. Phys.* **1989**, *65*, 2974.

[24] R. Hoelzl, M. Blietz, L. Fabry, R. Schmoke, in *Semiconductor Silicon 2002, PV 2002–2* (Eds: H. R. Huff, L. Fabry, S. Kishino), The Electrochemical Society Proceedings Series, Pennington, NJ, USA **2002**, p. 608.

[25] K. Sueoka, *J. Electrochem. Soc.* **2005**, *152*, G731.

[26] M. Hourai, T. Nagashima, H. Nishikawa, W. Sugimura, T. Ono, S. Umeno, *Phys. Status Solidi A* **2019**, *216*, 1800664.

[27] A. A. Istratov, E. R. Weber, *Appl. Phys. A* **1998**, *66*, 123.

[28] A. A. Istratov, C. Flink, H. Hieslmair, S. A. McHugo, E. R. Weber, *Mater. Sci. Eng. B* **2000**, *72*, 99.

[29] M. Hourai, T. Naridomi, Y. Oka, K. Murakami, S. Sumita, N. Fujino, T. Shiraiwa, *Jpn. J. Appl. Phys.* **1988**, *27*, L2361.

[30] M. W. Jenkins, *J. Electrochem. Soc.* **1977**, *124*, 757.

[31] M. B. Shabani, Y. Shiina, F. G. Kirscht, Y. Shimanuki, *Mater. Sci. Eng. B* **2003**, *102*, 238.

[32] S. Umeno, Y. Yanase, M. Hourai, M. Sano, Y. Shida, H. Tsuya, *Jpn. J. Appl. Phys.* **1999**, *38*, 5725.

[33] S. Sadamitsu, S. Umeno, Y. Koike, M. Hourai, S. Sumita, T. Shigematsu, *Jpn. J. Appl. Phys.* **1993**, *32*, 3675.

[34] K. Torigoe, T. Ono, K. Nakamura, *ECS J. Solid State Sci. Technol.* **2015**, *4*, Q110.

[35] A. A. Istratov, C. Flink, S. Balasubramanian, E. R. Weber, H. Hieslmair, S. A. McHugo, H. Hedemann, M. Seibt, W. Schröter, in *High Purity Silicon VI, PV 2000–17* (Eds: C. L. Claeys, P. Rai-Choudhury, M. Watanabe, P. Stallhofer, H. J. Dawson), The Electrochemical Society Proceedings Series, Pennington, NJ, USA **2000**, p. 258.

[36] A. A. Istratov, H. Hedemann, M. Seibt, O. F. Vyvenko, W. Schröter, T. Heiser, C. Flink, H. Hieslmair, E. R. Weber, *J. Electrochem. Soc.* **1998**, *145*, 3889.

[37] S. Shirasawa, K. Sueoka, T. Yamaguchi, K. Maekawa, *ECS J. Solid State Sci. Technol.* **2015**, *4*, P351.

[38] D. A. Ramappa, W. B. Henley, *Appl. Phys. Lett.* **1998**, *72*, 2298.

[39] M. Seibt, K. Graff, *J. Appl. Phys.* **1988**, *63*, 4444.

[40] J. K. Solberg, *Acta Cryst.* **1978**, *A34*, 684.